



Transportation Science

Publication details, including instructions for authors and subscription information:
<http://pubsonline.informs.org>

Capturing Dependency Among Link Boundaries in a Stochastic Dynamic Network Loading Model

Carolina Osorio, Gunnar Flötteröd

To cite this article:

Carolina Osorio, Gunnar Flötteröd (2015) Capturing Dependency Among Link Boundaries in a Stochastic Dynamic Network Loading Model. *Transportation Science* 49(2):420-431. <http://dx.doi.org/10.1287/trsc.2013.0504>

Full terms and conditions of use: <http://pubsonline.informs.org/page/terms-and-conditions>

This article may be used only for the purposes of research, teaching, and/or private study. Commercial use or systematic downloading (by robots or other automatic processes) is prohibited without explicit Publisher approval, unless otherwise noted. For more information, contact permissions@informs.org.

The Publisher does not warrant or guarantee the article's accuracy, completeness, merchantability, fitness for a particular purpose, or non-infringement. Descriptions of, or references to, products or publications, or inclusion of an advertisement in this article, neither constitutes nor implies a guarantee, endorsement, or support of claims made of that product, publication, or service.

Copyright © 2015, INFORMS

Please scroll down for article—it is on subsequent pages



INFORMS is the largest professional society in the world for professionals in the fields of operations research, management science, and analytics.

For more information on INFORMS, its publications, membership, or meetings visit <http://www.informs.org>

Capturing Dependency Among Link Boundaries in a Stochastic Dynamic Network Loading Model

Carolina Osorio

Department of Civil and Environmental Engineering, Massachusetts Institute of Technology, Cambridge, Massachusetts 02139,
osorioc@mit.edu

Gunnar Flötteröd

Department of Transport Science, KTH Royal Institute of Technology, 11428 Stockholm, Sweden,
gunnar.floetteroed@abe.kth.se

This work adds realistic dependency structure to a previously developed analytical stochastic network loading model. The model is a stochastic formulation of the link-transmission model, which is an operational instance of Newell's simplified theory of kinematic waves. Stochasticity is captured in the source terms, the flows, and, consequently, in the cumulative flows. The previous approach captured dependency between the upstream and downstream boundary conditions within a link (i.e., the respective cumulative flows) only in terms of time-dependent expectations without capturing higher-order dependency. The model proposed in this paper adds an approximation of full distributional stochastic dependency to the link model. The model is validated versus stochastic microsimulation in both stationary and transient regimes. The experiments reveal that the proposed model provides a very accurate approximation of the stochastic dependency between the link's upstream and downstream boundary conditions. The model also yields detailed and accurate link state probability distributions.

Keywords: stochastic network loading; queueing theory; dependency

History: Received: March 2012; revision received: April 2013; accepted: July 2013. Published online in *Articles in Advance* June 16, 2014.

1. Introduction

A *network loading model* describes how a time-dependent travel demand advances through a network. The demand is typically given in terms of time-dependent origin/destination (OD) flows and a route choice model. Given these inputs, the network loading model then captures the progression of the demand through the network, accounting for congestion and the resulting delays.

A *stochastic network loading model* does essentially the same, but it additionally accounts for uncertainty in the modeling (e.g., of source terms, flows, network parameters) and captures distributional information of the network states. This paper focuses on analytical stochastic (i.e., probabilistic) dynamic network loading models. The main technical limitation in developing such models is the dimensionality of the joint distribution, which is exponential in the number of spatial discretization units. Thus, the challenge is to approximate the dependency structure while deriving a computationally efficient approach.

In the following, we focus on the widely accepted kinematic wave model (KWM; see Lighthill and Witham 1955; Richards 1956). Both the KWM's original link model and its more recently developed node

models (e.g., Daganzo 1995; Lebacque 1996; Lebacque and Khoshyaran 2005; Tampere et al. 2011; Flötteröd and Rohde 2011; Corthout et al. 2012) are deterministic. They describe space/time average conditions but do not account for higher-order distributional information.

There has been a recent interest in the development of stochastic link models. Most studies have considered stochastic cell-transmission models (CTMs; see Boel and Mihaylova 2006; Sumalee et al. 2011; Jabari and Liu 2012). Boel and Mihaylova (2006) consider the sending and receiving functions of the CTM as random variables. The evaluation of the model involves computationally intensive sampling to estimate the main link performance measures. Jabari and Liu (2012) consider headways to be random variables. The fluid limit of their stochastic model is consistent with the CTM. This is also a simulation-based approach, where performance measure estimates are obtained via sampling. The stochastic CTM of Sumalee et al. (2011) allows for stochasticity in the sending and receiving functions and in the source terms. This model is analytical (i.e., not simulation based). The stochasticity results from adding noise in the form of a second-order wide-sense stationary process to otherwise deterministic model variables. Jabari

and Liu (2012) detail the limitations of using such types of noise terms.

Let us also briefly comment on the kinetic approach to stochastic traffic flow modeling. Here, one starts out from a probabilistic description of individual vehicle interactions, which is typically solved by extracting dynamic equations for the first moments (in particular, mean values and variances) of aggregate traffic characteristics (e.g., Tampere, van Arem, and Hoogendoorn 2003). To derive operational formulations, the assumption of “vehicular chaos” is typically made, meaning that the states of interacting vehicles are stochastically independent. Nelson and Kumar (2006) elaborate on the implications of omitting such dependencies. It appears that the complexity of kinetic models with realistic stochastic dependency structures has so far precluded their implementation in nontrivial network contexts (Helbing 2001).

Osorio, Flötteröd, and Bierlaire (2011) recently proposed a stochastic formulation of the link-transmission model of Yperman, Tampere, and Immers (2007), which is an operational instance of Newell’s (1993) simplified theory of kinematic waves. Newell’s model can, in turn, be derived from the variational theory of Daganzo (2005). The queueing-theoretical model of Osorio, Flötteröd, and Bierlaire accommodates stochastic source terms and flows across nodes. It is a (vehicle)-discretized, stochastic instance of the KWM, whereas the aforementioned stochastic CTMs constitute stochastic instances of (space)-discretized KWMs. That is, only the model of Osorio, Flötteröd, and Bierlaire is *directly* derived from the KWM.

The present paper adds important dependency structure to this model, hereafter referred to as the *basic model*. The basic model exhibits the following additional features.

1. It is analytical. It captures the evolution of link state distributions through differentiable equations. Thus, the approach does not require computationally costly sampling to obtain distributional estimates. This approach allows for obtaining valuable insights into stochastic network dynamics. It also provides a differentiable description of these dynamics, which can be exploited when applying efficient optimization or calibration routines, e.g., for the design of signal control strategies (Osorio and Bierlaire 2013) or the estimation of OD matrices (Flötteröd, Bierlaire, and Nagel 2011).

2. The basic model represents the flow transmissions across a network node (connection of upstream and downstream links) in terms of a multivariate Poisson process. The node model yields a joint distribution of the downstream boundary conditions of the node’s upstream link and the upstream boundary conditions of the node’s downstream link.

3. The basic model represents a homogeneous link segment by two finite-capacity queues that constitute stochastic counterparts of the cumulative curves used in Newell’s (1993) simplified KWM, and it coincides with a discretized version of Newell’s model when the randomness in all involved processes vanishes. That is, the basic link model is derived from the KWM (Newell 1993; Yperman, Tampere, and Immers 2007).

4. The basic model captures the dependency between a single link’s upstream boundary conditions and the same link’s downstream boundary conditions merely in terms of time-dependent expectations, but it ignores higher-order dependencies. This implies that dependency between upstream and downstream boundary conditions in a single link is not captured beyond what a deterministic model could describe.

Item 4 constitutes the main simplification in the basic model, which this paper overcomes. The presentation therefore focuses on the joint modeling of boundary conditions within a link. Details on how across-node correlations (i.e., correlations with links further up- or downstream) are captured appear in Osorio, Flötteröd, and Bierlaire (2011). It should be noted that none of the aforementioned stochastic CTMs provides analytical expressions for the joint distribution of multiple cells: Boel and Mihaylova (2006) and Jabari and Liu (2012) resort to simulation; Sumalee et al. (2011) model the states of adjacent cell pairs as independent random variables.

The remainder of this paper is organized as follows: §2 recalls the basic link model. Section 3 describes how realistic dependency structure is added, leading to the proposed new model. Comprehensive experiments are described in §4, where the distributional information extracted from the analytical model is compared with distributional estimates obtained via simulation. Finally, §5 concludes and gives an outlook on further research questions.

2. Basic Link Model

We briefly recall the original link model of Osorio, Flötteröd, and Bierlaire (2011). The presentation given here follows a different path than the original work in that it first recalls an operational formulation (Yperman, Tampere, and Immers 2007) of Newell’s (1993) simplified KWM and then formulates the stochastic model as a distributed version of Newell’s model.

Yperman, Tampere, and Immers (2007) phrase this model within the sending/receiving function framework of Daganzo (1994) and Lebacque (1996). This framework postulates that, at any interface within the network, the instantaneously transmitted flow is the minimum of an upstream sending function and a downstream receiving function, reflecting the

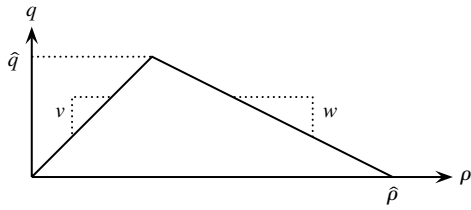


Figure 1 Deterministic Fundamental Diagram Resulting from Original Two-Queue System

KWM's principle of local flow maximization (Ansorge 1990). The embedding of a link in a network model hence requires a link model that defines, at every time instant t , a receiving function $R(t)$ (respectively, a sending function $S(t)$) that reflects the boundary conditions the link provides to its upstream node (respectively, downstream node).

Assuming a triangular fundamental diagram as shown in Figure 1, having free flow velocity v , backward wave speed w (negative), flow capacity \hat{q} , and jam density $\hat{\rho}$, Yperman, Tampere, and Immers (2007) present the following equations for a discrete-time simulation of the KWM (detailed derivations can be found in Yperman 2007):

$$R(t) = \min \left\{ N \left(L, t + \delta - \frac{L}{|w|} \right) + \hat{\rho}L - N(0, t), \hat{q}\delta \right\} \quad (1)$$

$$S(t) = \min \left\{ N \left(0, t + \delta - \frac{L}{v} \right) - N(L, t), \hat{q}\delta \right\}, \quad (2)$$

where $R(t)$ is the amount of flow the link can receive at time instant t during the next time interval of length δ , $S(t)$ is the respective sending flow, and $N(x, t)$ is the cumulative flow having passed location x at time t , with $x \in [0, L]$ in the link of length L . The Courant-Friedrichs-Lewy condition requires $\delta \leq L/v$ to hold. See, for instance, Yperman (2007) for a detailed discussion of the possible wave configurations given a triangular fundamental diagram and Nagel and Nelson (2005) for a discussion of its empirical validity.

Defining the two quantities

$$UQ(t) = N(0, t) - N(L, t + \delta - L/|w|) \quad (3)$$

and

$$DQ(t) = N(0, t + \delta - L/v) - N(L, t) \quad (4)$$

allows us to rewrite (1) and (2) as follows:

$$R(t) = \min \{ \hat{\rho}L - UQ(t), \hat{q}\delta \} \quad (5)$$

$$S(t) = \min \{ DQ(t), \hat{q}\delta \}. \quad (6)$$

Formally, $UQ(t)$ and $DQ(t)$ are just summary representations of differences in cumulative flows. However, they also allow for a tangible interpretation of

these otherwise rather abstract cumulative flow differences. For this, $UQ(t)$ is interpreted as the number of vehicles in a finite-capacity *upstream queue* (UQ) that keeps track of the upstream boundary conditions *within* the link, and $DQ(t)$ is interpreted as the number of vehicles in a finite-capacity *downstream queue* (DQ) that keeps track of the downstream boundary conditions *within* the link.

Allow both queues to hold at most $\hat{\rho}L$ vehicles. The receiving function in (5) is hence limited by the available space in UQ, which is $\hat{\rho}L - UQ(t)$. This means that the link behaves *as if* UQ was embedded within its upstream end and *as if* vehicles trying to enter the link actually tried to enter UQ. Further, the sending function in (6) is limited by the number of vehicles in DQ, which is $DQ(t)$. This means that the link behaves *as if* DQ was embedded within its downstream end and *as if* vehicles leaving the link actually left DQ. (Charypar (2008) describes essentially the same approach in a microsimulation framework but without any analytical considerations.)

This interpretation carries further. Equations (3) and (4) can be recursively written as

$$UQ(t) = UQ(t - \delta) + \delta[q^{\text{in}}(t - \delta) - q^{\text{out}}(t - L/|w|)] \quad (7)$$

$$DQ(t) = DQ(t - \delta) + \delta[q^{\text{in}}(t - L/v) - q^{\text{out}}(t - \delta)], \quad (8)$$

where $q^{\text{in}}(t)$ is the link's instantaneous inflow rate at time t , $q^{\text{out}}(t)$ is the instantaneous outflow rate, and both quantities are held constant throughout a time step of duration δ , consistent with the underlying framework of Yperman, Tampere, and Immers (2007). Equation (7) indicates that the change in UQ during $[t - \delta, t]$ is given by the difference between

(i) the flow that entered the link during that time, and

(ii) the flow that left the link during $[t - L/|w|, t - L/|w| + \delta]$.

Similarly, Equation (8) indicates that the change in DQ during $[t - \delta, t]$ is given by the difference between

(i) the flow that entered the link during $[t - L/v, t - L/v + \delta]$, and

(ii) the flow that left the link during that time.

That is, UQ and DQ evolve through time *as if* the link in- and outflows actually entered the respective queues. It needs to be reiterated, though, that UQ and DQ are merely intuitive representations of the boundary conditions provided by the link to its up- and downstream nodes.

Figure 2 shows the fictitious embedding of UQ and DQ within the link. The lower path (solid arrows) represents the actual mass transfer: flow enters the link, is delayed by L/v time units (corresponding to the free-flow travel time), and then becomes available for departure in DQ. The upper path (dashed

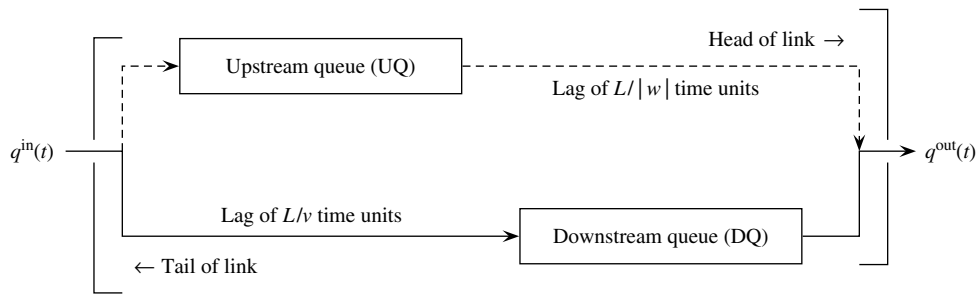


Figure 2 Original Two-Queue System

arrows) captures how vehicle departures eventually enable new vehicle entries, in that flows that have departed from DQ are delayed by $L/|w|$ time units (corresponding to the time it takes a kinematic backward wave to traverse the link) before they are removed from UQ.

The stochastic link model results from a stochastic modeling of UQ and DQ, relying on finite-capacity queueing theory, where the evolution of the distribution of the number of vehicles in either queue is tracked through time. The dynamics of these queues are guided by time-dependent arrival and service rates as well as the probabilities of the queues being perfectly empty (i.e., being unable to send more flow) or perfectly full (i.e., being unable to receive more flow). Since UQ and DQ represent differences in cumulative flows, this approach corresponds to Newell’s (1993) model with stochastic cumulative curves.

Assume a time-dependent Poisson arrival process with intensity $\lambda(t)$ (i.e., a nonhomogeneous Poisson process) at the upstream end of the considered link, where $\lambda(t) \leq \hat{q}$ to capture the second constraint in Equation (1). That is, interarrival times of vehicles to the link are exponentially distributed. This captures uncertainty in the source term (or, in a network context, in the demand from upstream). The probability that an arrival at time t encounters an available space in UQ is $P(\text{UQ}(t) < \ell)$, where ℓ is the link’s space capacity (corresponding to a rounded version of $\hat{q}L$). Allowing for losses (which would translate into spill-back in the full-node model not considered here), the effective inflow becomes $q^{\text{in}}(t) = \lambda(t)P(\text{UQ}(t) < \ell)$.

Furthermore, assume exponentially distributed service times at the downstream end of the link with rate $\mu(t) \leq \hat{q}$ to capture the second constraint in Equation (2), where $\mu(t)$ can be interpreted as a downstream capacity constraint (which in a network embedding would capture, among other things, spill-back from downstream). Distributed service times may capture a distribution of headways across vehicles or stochastic flow interactions in the downstream node, the latter being possibly due to a gap acceptance distribution. The probability that there are vehicles ready to leave the link is given by the probability

that there are vehicles in DQ. Thus, the outflow of the link is given by $q^{\text{out}}(t) = \mu(t)P(\text{DQ}(t) > 0)$.

The basic model captures uncertainties in upstream demand patterns and downstream supply conditions. Specifically, this model assumes arrivals to arise from a Poisson process. Two common criticisms of this assumption are mitigated by features of the present model, which are absent in other Markovian-type road traffic models. As discussed in Osorio, Flötteröd, and Bierlaire (2011), the *dynamics* allow the capture of temporal dependency effects (e.g., platooning) deterministically through the joint dynamics of the time-dependent rates of all involved Poisson processes. The *finite-capacity* assumption of this model ensures that unrealistically high flows do not arise. Such flows could arise in an infinite-capacity queue setting because of the Poisson distribution’s fat right tail. Ultimately, these assumptions will require empirical justification.

This link model is a simplification in the sense that UQ and DQ are modeled independently. To clarify this, let the *lagged inflow* $\text{LI}(t)$ at time t be the stochastic amount of flow that has entered the link between $t - L/v$ and t . In Figure 2, this corresponds to the flow on the lower left path, which has already entered the link but has not yet entered DQ. Further, let the *lagged outflow* $\text{LO}(t)$ at time t be the stochastic amount of flow that has left the link between $t - L/|w|$ and t . In Figure 2, this corresponds to the flow on the top right path, which has already left the link but has not yet left UQ. Mass conservation then requires

$$\text{LI}(t) + \text{DQ}(t) = \text{UQ}(t) - \text{LO}(t) \quad (9)$$

to hold. Both sides denote the number of vehicles on the link at time t , such that a substantial dependency between the distribution of UQ and DQ can be expected.

The remainder of this paper develops and analyzes an improved link model formulation that almost perfectly captures this dependency while maintaining consistency with the network modeling framework of Osorio, Flötteröd, and Bierlaire (2011).

3. New Link Model

The main difficulty when trying to capture a joint distribution of UQ and DQ is the fact that these evolve in reaction to the same inflows and outflows, but evaluate these flows with different time lags.

We assume a discrete model where k is the time index, k^{fwd} is a rounded version of L/v , k^{bwd} is a rounded version of $L/|w|$, and ℓ is a rounded version of $\hat{\rho}L$. A joint distribution of all time-lagged model variables would result in an exponential state space increase as the involved time lags get larger.

The proposed solution to this problem is to add only two additional dimensions to the (UQ, DQ) state space, which are called the *lagged inflow queue* (LI) and the *lagged outflow queue* (LO). The LI queue captures, at an aggregate level, the distribution of all link entries that have not yet reached DQ; cf. Equation (8). Symmetrically, the LO queue captures, at an aggregate level, the distribution of all link exits that have not yet been removed from UQ; cf. Equation (7). Modeling a joint evolution of a four-dimensional state space (UQ, LI, DQ, LO) is expected to capture relevant aspects of the dependency between UQ and DQ.

Figure 3 gives an overview. In discrete time, the lags of inflows and outflows correspond to moving them through a sequence of k^{fwd} (respectively, k^{bwd}) buffers. LI (respectively, LO) contains the sum of the lagged

inflows (respectively, outflows) in the corresponding buffers. That is, each dotted box contains three alternative ways of representing a lag: the original lag in continuous time, the discrete-time representation as a series of buffers, and the aggregation into one single queue.

Let $UQ(t; k)$ denote the number of vehicles in UQ at continuous time t within time interval k of duration δ . Similarly, we define $LI(t; k)$, $DQ(t; k)$, and $LO(t; k)$. At a given point in time, we have

$$UQ(t; k) = DQ(t; k) + LI(t; k) + LO(t; k). \quad (10)$$

Let us emphasize the purpose of each of these queues. DQ represents the number of vehicles that could possibly leave the link. LI represents the number of vehicles that have entered the link but are not yet available for departure because of the finite link traversal time. LO represents the number of “spaces” that correspond to departures from the link that, because of the finite backward wave speed, have not yet propagated to the link’s upstream end. Thus, UQ in (10) represents all vehicles on the link *plus* those vehicles that have recently left the link but whose available space has yet to become available for use upstream.

We only model the joint evolution of the three independent queues (LI, DQ, LO), noting that the state of

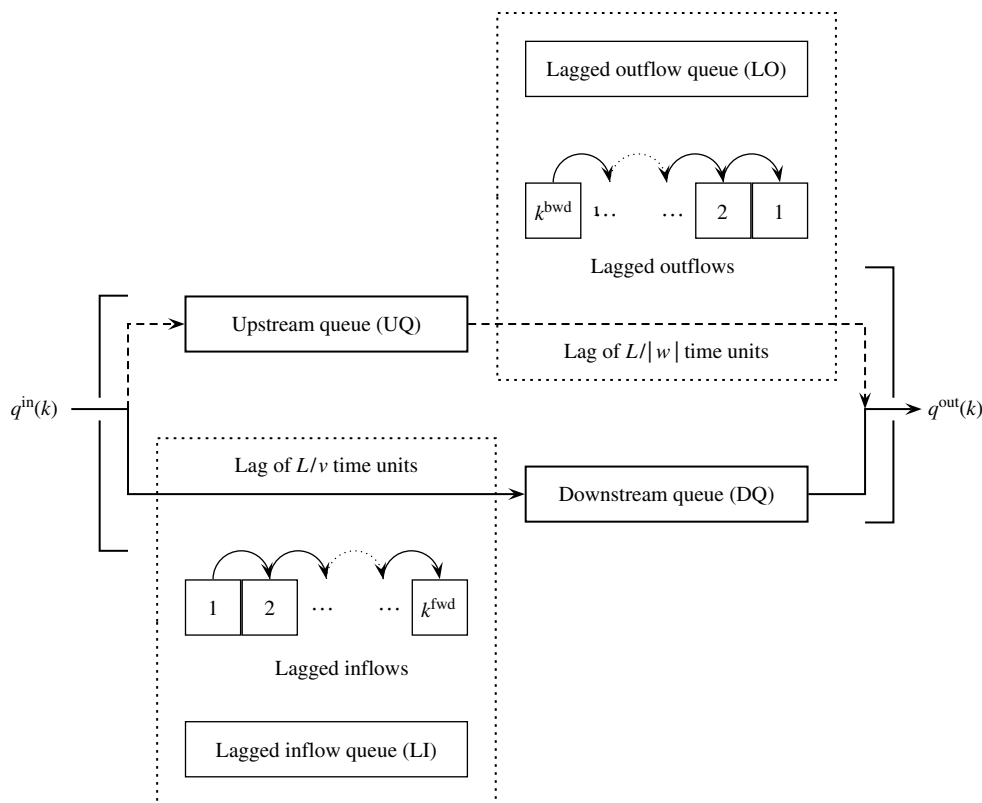


Figure 3 Lagged Inflow/Outflow Buffers, Aggregated into a Four-Queue System

the fourth queue can be deduced from (10). The state space of a link consists of all feasible values of this triplet of random variables. It is defined as

$$\{(li, dq, lo) \in \mathbb{N}^3, li + dq + lo \leq \ell\}. \quad (11)$$

Let $p(t; k)$ denote the joint transient probability distribution of (LI, DQ, LO) at continuous time t within time interval k of duration δ . The evolution of this distribution is given in continuous time t from 0 to δ by the following linear system of differential equations (see, for instance, Reibman 1991):

$$\frac{dp(t; k)}{dt} = p(t; k)Q(k) \quad \forall t \in [0, \delta], \quad (12)$$

where $p(t; k)$ is a probability vector and $Q(k)$ is a square matrix, known as the transition rate matrix, which is described below. Initial conditions ensure continuity at the beginning of the time interval:

$$p(0; k) = p(\delta; k - 1). \quad (13)$$

The general solution to Equations (12) and (13) is given by

$$p(t; k) = p(0; k)e^{Q(k)t} \quad \forall t \in [0, \delta]. \quad (14)$$

Equation (14) is a discrete-time differentiable expression, which guides the transition of the queue distributions from one time step to the next. It holds under the assumption of constant link boundary conditions during a time step; i.e., $Q(k)$ is constant during time interval k . This assumption was already introduced in the framework of §2.

For a given system of queues, $Q(k)$ is a function of the arrival rates and service rates of each of the queues. This matrix contains the transition rates between all pairs of states. The nondiagonal elements, $Q(k)_{sj}$ for $s \neq j$, represent the rate at which the transition from state s to state j takes place. The diagonal elements are defined as $Q(k)_{ss} = -\sum_{j \neq s} Q(k)_{sj}$. Thus, $-Q(k)_{ss}$ represents the rate of departure from state s .

The nondiagonal and nonnull elements of the transition rate matrix are given in Table 1. Assume an initial state of (LI, DQ, LO) equal to (li, dq, lo) . The first row of the table describes arrivals to the link. They occur with rate $\lambda(k)$ and may enter the link as long as $li + dq + lo < \ell$; i.e., they may enter as long as UQ is less than the space capacity ℓ . Flow from

LI to DQ (second row of the table) is transmitted with rate $\mu^{LI}(li; k)$, and this can occur as long as LI is nonempty ($li > 0$). The third row describes departures from the link. They occur at rate $\mu^{DQ}(k)$ as long as DQ is nonempty. The last row describes departures from LO, which occur at rate $\mu^{LO}(lo; k)$.

The link dynamics are described via the queueing parameters $\lambda(k)$,

$$\{\mu^{LI}(li; k)\}_{li=1, \dots, \ell}, \mu^{DQ}(k), \text{ and } \{\mu^{LO}(lo; k)\}_{lo=1, \dots, \ell},$$

which are derived in the following:

- $\lambda(k)$ is exogenous to the single-link model considered here.
- $\mu^{DQ}(k)$ defines the rate at which flow may leave the link. It also is considered exogenous in this paper.
- $\mu^{LI}(li; k)$ is the rate at which the LI queue discharges into DQ, given that LI contains li vehicles.

At the beginning of time interval k , queue LI contains all arrivals to the link at time intervals $k - k^{fwd}$, $k - k^{fwd} + 1, \dots, k - 1$. It represents a sequence of k^{fwd} buffer cells, where cell j contains the entries to the link during time interval $k - j$. The number of vehicles in LI is the sum of the vehicles in these k^{fwd} cells. The vehicles that can leave LI during time interval k are those that are in LI's last (i.e., most downstream) cell, which is denoted by LLI. That is, LLI represents the k^{fwd} th buffer cell of LI. Hereafter, we use $LI(k)$ to denote $LI(0; k)$, i.e., the number of vehicles in LI at the beginning of time interval k ; an according notation is used for all other time-dependent quantities as well.

The flow from LI to DQ during time interval k is given by the number of vehicles in LLI at the beginning of time interval k , i.e., $LLI(k)$. We proceed by deriving $E\{LLI(k) \mid LI(k) = li\}$, which is the expected flow transferred from LLI into DQ during time interval k , given that LI contains li vehicles.

The arrival process to the link during time interval k is a Poisson process with rate $\lambda(k)$. Arrivals may enter the link as long as it has not spilled back. This occurs with probability $P(UQ(k) < \ell)$. Thus, the vehicles enter the link according to a Poisson process with a rate

$$q^{in}(k) = \lambda(k)P(UQ(k) < \ell), \quad (15)$$

where $q^{in}(k)$ represents the expected inflow to the link during time interval k . Updating the arrival rates across time intervals allows the model to account for temporal dependency between arrivals. This occurs, for instance, in a network context without losses, where vehicles that were blocked (i.e., could not enter) in previous time steps enter in later time steps. Additionally, temporal dependence is introduced through UQ, which modulates the inflow through its probability of not being full in Equation (15) and evolves relatively slowly along the time axis.

Table 1 Transition Rates Between Queues LI, DQ, and LO

Initial state s	New state j	Rate $Q(s, j; k)$	Condition
(li, dq, lo)	$(li + 1, dq, lo)$	$\lambda(k)$	$li + dq + lo < \ell$
(li, dq, lo)	$(li - 1, dq + 1, lo)$	$\mu^{LI}(li; k)$	$li > 0$
(li, dq, lo)	$(li, dq - 1, lo + 1)$	$\mu^{DQ}(k)$	$dq > 0$
(li, dq, lo)	$(li, dq, lo - 1)$	$\mu^{LO}(lo; k)$	$lo > 0$

The only simplifying assumption made here and in the following is to neglect the stochastic temporal dependence between inflows (and, as explained later, outflows) at different time steps. The experiments of §4 demonstrate the very minor effect of this approximation. Given this, the arrivals to each inflow buffer cell constitute independent Poisson processes with corresponding rates $q^{\text{in}}(k-1), \dots, q^{\text{in}}(k-k^{\text{fwd}})$, and $\text{LI}(k)$ is the sum of these independent processes. Thus, the conditional distribution of $\text{LLI}(k)$ given that $\text{LI}(k) = li$ is binomial $B(li, r(k))$, with

$$r(k) = \frac{q^{\text{in}}(k-k^{\text{fwd}})}{\sum_{j=1}^{k^{\text{fwd}}} q^{\text{in}}(k-j)} \quad (16)$$

being the probability of encountering a randomly selected vehicle from $\text{LI}(k)$ in $\text{LLI}(k)$. For a derivation of this result (i.e., the binomial distribution and its corresponding parameters), see §2.12.4 of Larson and Odoni (1981).

In consequence,

$$E\{\text{LLI}(k) \mid \text{LI}(k) = li\} = li \cdot r(k). \quad (17)$$

The service rate $\mu^{\text{LI}}(li; k)$ can now be derived. By definition, the service rate is the inverse of the expected time between successive departures from LI. To derive this expectation, we observe that departures from LI form a Poisson process, and the expected number of departures given that LI has li vehicles is given by $E\{\text{LLI}(k) \mid \text{LI}(k) = li\}$.

Given that m events of a Poisson process have occurred during a fixed time interval δ , then interevent times are independently, uniformly distributed over the fixed time interval of interest with expected interarrival time δ/m (see, for instance, Larson and Odoni 1981, §2.12.3). In our case, $m = E\{\text{LLI}(k) \mid \text{LI}(k) = li\}$, such that the service rate becomes

$$\mu^{\text{LI}}(li; k) = \frac{li}{\delta} \cdot \frac{q^{\text{in}}(k-k^{\text{fwd}})}{\sum_{j=1}^{k^{\text{fwd}}} q^{\text{in}}(k-j)}. \quad (18)$$

- $\mu^{\text{LO}}(lo; k)$ is the rate at which “spaces” resulting from downstream vehicle departures become available upstream. Queue LO contains all departures from DQ at time intervals $k-k^{\text{bwd}}, k-k^{\text{bwd}}+1, \dots, k-1$. Symmetrically to the derivation that led to Equation (18), the departure rate from LO given that LO contains lo vehicles is

$$\mu^{\text{LO}}(lo; k) = \frac{lo}{\delta} \cdot \frac{q^{\text{out}}(k-k^{\text{bwd}})}{\sum_{j=1}^{k^{\text{bwd}}} q^{\text{out}}(k-j)}. \quad (19)$$

In summary, the overall link model is solved by repeated evaluations of Equation (14), using the exogenous parameters $\lambda(k)$ and $\mu^{\text{DQ}}(k)$ and the endogenous transmission rates defined in Equations (18) and (19). The linkage between Equation (14) and these rates is given in Table 1.

4. Experiments

A single-lane link with parameters shown in Table 2 is considered. Nine experiments are conducted, combining three different arrival rate profiles and three different link lengths (and, hence, different space capacities and forward/backward lags).

Each experiment starts with an initially empty link at time zero and runs for 3,000 one-second time steps. The arrival profiles are displayed in Table 3. Profile 131 (respectively, 151) corresponds to a step change from undercritical to marginally critical (respectively, overcritical) conditions and back. Profile 353 corresponds to a step change from marginally critical to overcritical conditions and back.

The considered space capacities are $\ell = 10, 20, 30$, resulting in link lengths $L = 50, 100, 150$ m, forward time lags $k^{\text{fwd}} = 5, 10, 15$, and backward time lags $k^{\text{bwd}} = 10, 20, 30$. Table 4 labels the experiments for the resulting nine parameter combinations as concatenations of the respective arrival profile and space capacity.

Particular attention is paid in the following to the stochastic dependency between up- and downstream conditions within the link, corresponding to dependency between UQ and DQ. For this, the results of the proposed analytical model are compared to empirical distributions obtained from 10^6 replications of an event-based microsimulation.

Table 2 Link Parameters

Parameter	Value
v	36 km/h
w	−18 km/h
\hat{q}	200 veh/km
\hat{q}	2,400 veh/h = 0.67 veh/s
$\mu(k)$	1,080 veh/h = 0.3 veh/s
$\lambda(k)$	Varies by experiment
$\ell, L, k^{\text{fwd}}, k^{\text{bwd}}$	Varies by experiment

Table 3 Arrival Rate Profiles $\lambda(k)$ (in Vehicles per Second)

Profile	Time interval k		
	[0, 999]	[1,000, 1,999]	[2,000, 2,999]
Profile 131	0.1	0.3	0.1
Profile 151	0.1	0.5	0.1
Profile 353	0.3	0.5	0.3

Table 4 Experiments

ℓ	λ -profile		
	131	151	353
10	“Exp131 Cap10”	“Exp151 Cap10”	“Exp353 Cap10”
20	“Exp131 Cap20”	“Exp151 Cap20”	“Exp353 Cap20”
30	“Exp131 Cap30”	“Exp151 Cap30”	“Exp353 Cap30”

This microsimulation implements only a UQ and a DQ. It does not resort to the LI and LO approximation but instead explicitly implements the time lags experienced by vehicles entering the link until they reach DQ and by spaces becoming available as a result of exiting vehicles until they reach UQ. The stochasticity of the arrival and service process is explicitly simulated by drawing corresponding random numbers. That is, the microsimulation implements an instance of the proposed model that comes with no approximations of the time lags—at the cost of being able to only draw from the underlying distributions (as opposed to an analytical approach). Because the microsimulation perfectly captures all dependencies, it serves as a benchmark for the analytical model.

Figure 4 shows for all nine experiments the evolution of the correlation between UQ and DQ over time. The crosses represent results from the analytical model, and the circles represent results from the event-based simulation. Figure 5 shows in greater detail the transient dynamics of the correlation around second 1,000; Figure 6 shows this around second 2,000. As a first impression, the deviations between the simulation and the analytical model are visually negligible, indicating an excellent overall fit.

Table 5 contains the stationary correlations between UQ and DQ for the three space capacities $\ell = 10, 20, 30$ and the three stationary arrival rates $\lambda = 0.1, 0.3, 0.5$ veh/s. Figure 7, panels (a), (g), and (d) show the corresponding (UQ, DQ) distributions for $\ell = 30$, obtained with the analytical model. The correlation values can be interpreted based on the joint distributions in the following way:

- All correlations are positive and quite large. This is plausible given that both UQ and DQ represent aspects of the link’s occupancy and have substantial overlap; cf. also Equation (10).
- For each given space capacity ℓ , the correlation is in marginally critical conditions higher than in under- or overcritical conditions. Under- and overcritical conditions differ from marginally critical conditions in this regard because Equation (10) implies that UQ is always fuller than DQ. In undercritical conditions, this limits joint downwards fluctuations of UQ and DQ because DQ is already close to zero; the (UQ, DQ) distribution is truncated at $DQ = 0$ in Figure 7, panel (a). In overcritical conditions, this limits joint upwards fluctuations because UQ is already close to ℓ ; the (UQ, DQ) distribution is truncated at $UQ = \ell$ in Figure 7, panel (d). In marginally critical

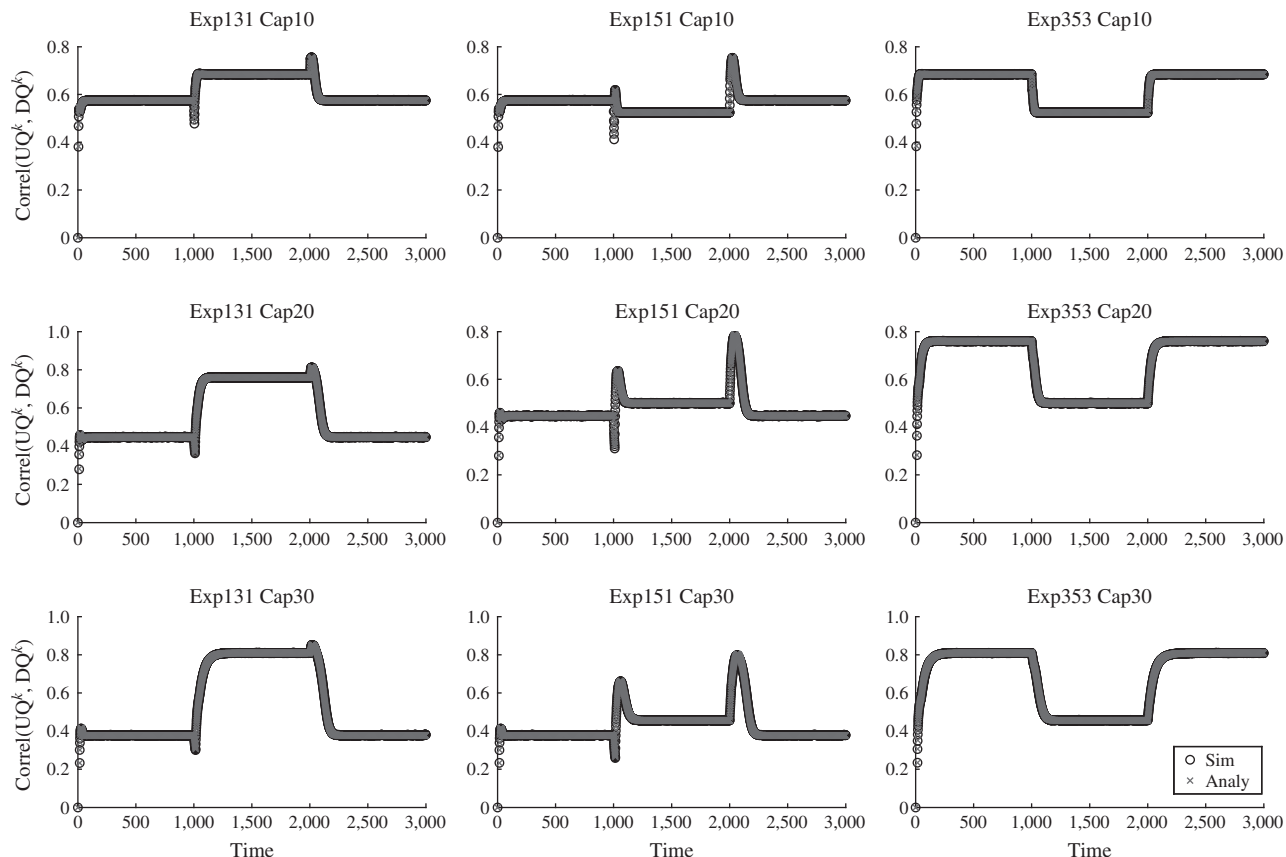


Figure 4 Correlation Between UQ and DQ Over Time

Downloaded from informs.org by [73.17.150.208] on 04 June 2015, at 12:46. For personal use only, all rights reserved.

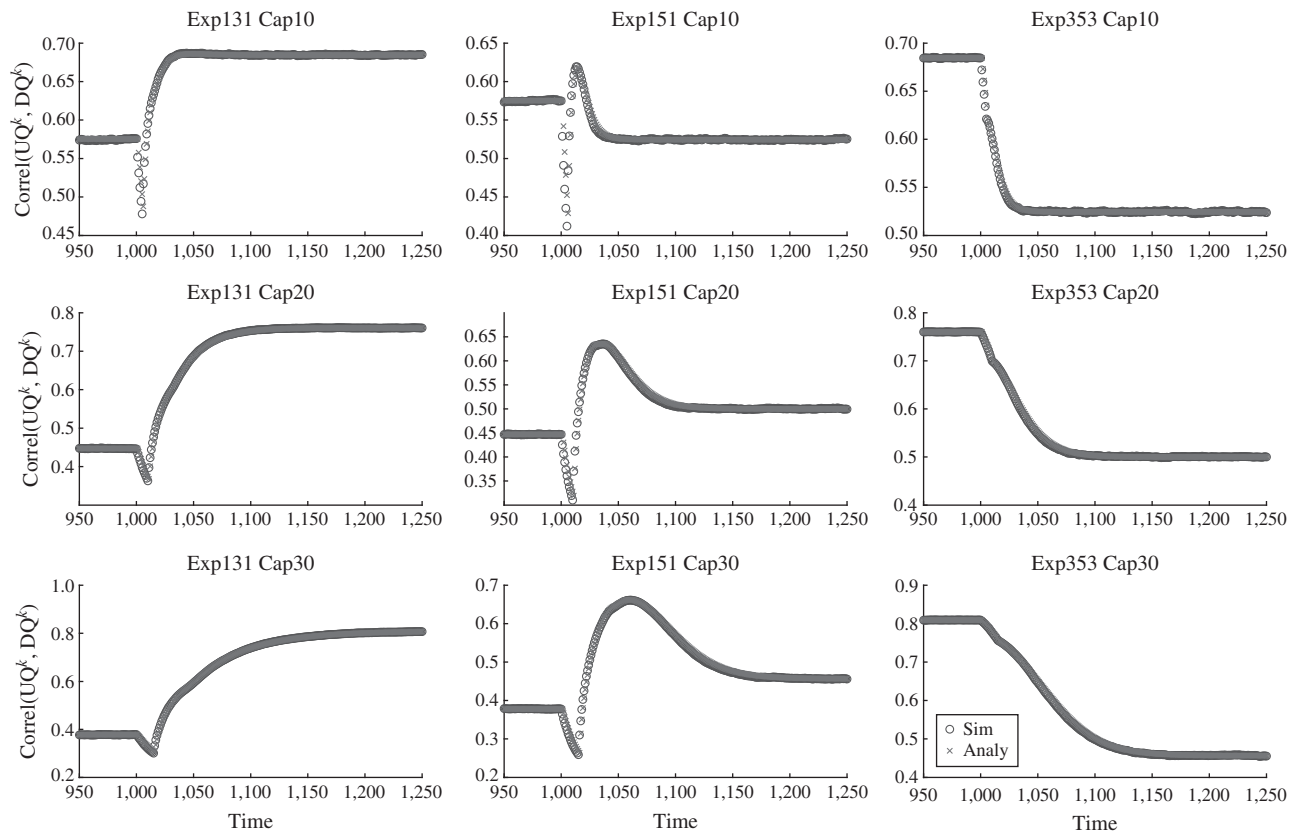


Figure 5 Correlation Between UQ and DQ During the Transition Around Second 1,000

conditions, the probability of these bounds taking effect is relatively low, allowing joint fluctuations of UQ and DQ to occur most freely in Figure 7, panel (g).

- For $\lambda = 0.1$ and 0.5 veh/s, the correlation decreases with increasing ℓ . This is so because in undercritical (respectively, overcritical) conditions, DQ (respectively, UQ) dictates the link dynamics, and the respective other queue follows. The longer the link is, the more room exists for independent fluctuations of the queues, resulting in reduced correlation. In terms of Equation (10), the LI+LO addend of $UQ = DQ + (LI + LO)$ increases relative to and somewhat independently of DQ, moving away from what would be a perfect $UQ = DQ$ dependency.

- For $\lambda = 0.3$ veh/s, the correlation increases with increasing ℓ . As explained before, the distributions of UQ and DQ evolve most freely in marginally critical conditions. Indeed, Figure 7, panel (g) reveals that the (UQ, DQ) distribution stretches in marginally critical conditions all the way from undercritical to overcritical conditions. As the link gets longer, this distribution stretches even further, resulting in the observed increase in correlation.

Figure 5 (respectively, Figure 6) provides a more detailed evaluation of the correlation dynamics during the transient periods around second 1,000 (respectively, 2,000). These transitions are captured very

accurately by the analytical model. Figure 7 shows snapshots of the (UQ, DQ) distribution for $\ell = 30$ during stationarity and the times of largest correlation under- and overshoot. Here, one observes the following.

- For second 1,000 and arrival profile 131 (first column in Figure 5), the correlation undershoots before attaining its new stationary value. These dynamics are reflected by the sequence of (UQ, DQ) distributions shown in Figure 7, panels (a), (f), and (g). The undershoot can be explained by UQ starting to increase k^{fwd} time steps before DQ, such that UQ initially changes independently of DQ. The (UQ, DQ) distribution first stretches out only horizontally before also expanding vertically. Eventually, this effect ceases as the two queues synchronize again. Consistent with this, the time of maximum undershoot coincides with the respective forward time lag k^{fwd} .

- For second 1,000 and arrival profile 151 (second column in Figure 5), the correlation first undershoots and then overshoots before attaining its new stationary value. These dynamics are reflected by the sequence of (UQ, DQ) distributions shown in Figure 7, panels (a)–(d). The undershoot is explained in the previous item (initial horizontal expansion of (UQ, DQ) distribution from Figure 7, panels (a) and (b)). The overshoot results because, whatever the initial (most

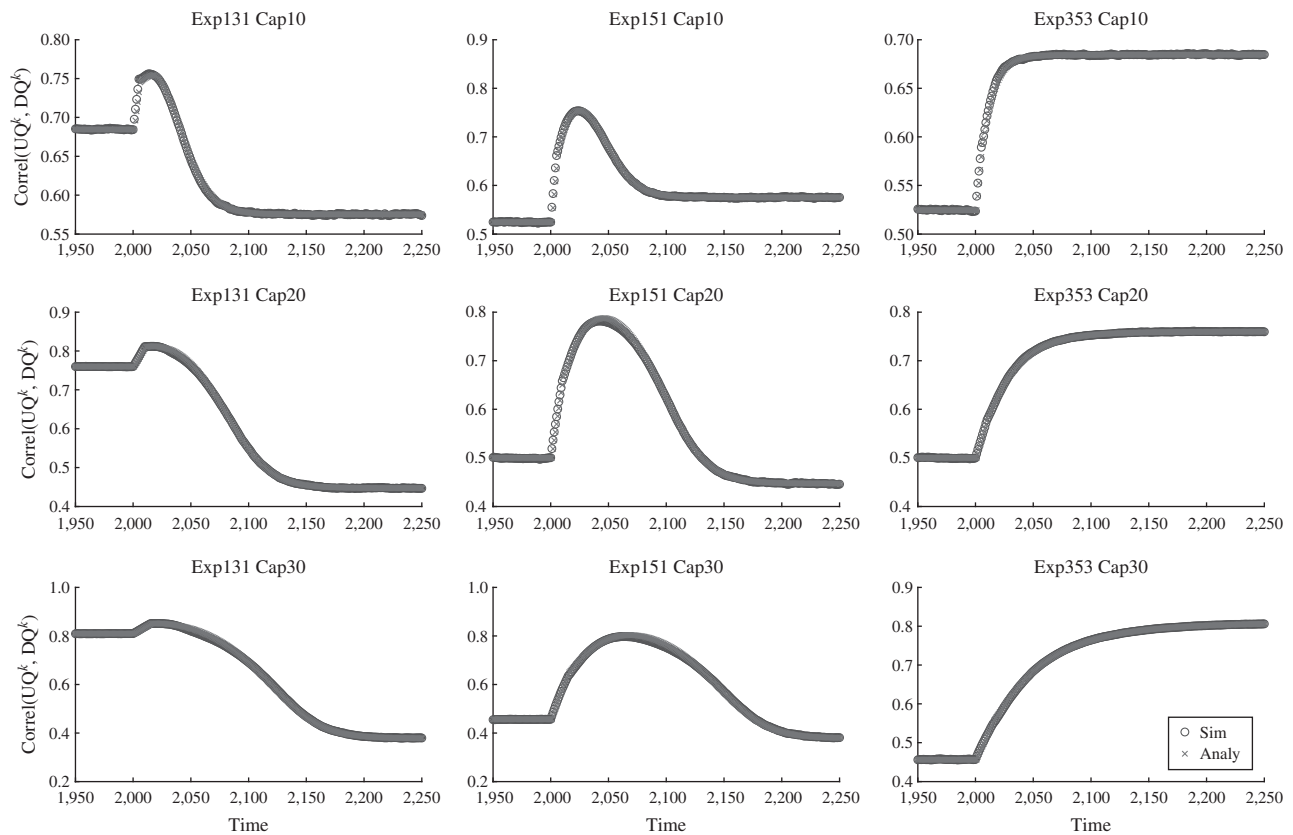


Figure 6 Correlation Between UQ and DQ During the Transition Around Second 2,000

likely, upwards) fluctuation of UQ is, the same fluctuation reaches DQ after k^{fwd} time steps. The relatively empty DQ is able to follow quite freely UQ’s earlier fluctuation. This is reflected by the diagonal stretch of the (UQ,DQ) distribution in Figure 7, panel (c). Eventually, the upper bound on UQ then takes effect, reducing the probability of joint fluctuations, which results in Figure 7, panel (d).

- For second 2,000 and arrival profiles 131 and 151 (first and second columns in Figure 6), the correlation overshoots before attaining its new stationary value. These dynamics are reflected by the sequence of (UQ, DQ) distributions shown in Figure 7, panels (g), (h), and (a) and (d), (e), and (a). The overshoot in arrival profile 151 can be explained by the link going all the way from over- to undercritical conditions, passing through a transient state of marginal criticality shown in Figure 7, panel (e). The transient overshoot

in arrival profile 131; cf. Figure 7, panel (h), exceeds the already extreme correlation in marginally critical stationary conditions, cf. Figure 7, panel (g). A careful comparison of these two figures reveals that the transient distribution is slightly narrower than the stationary distribution.

- For arrival profile 353 (last column in Figures 5 and 6), there are no over- or undershoots. In marginally critical and overcritical conditions, UQ takes at least partial effect on the link dynamics. Because the change in boundary conditions also occurs upstream, the immediate reaction of UQ absorbs the link dynamics that in the previous cases resulted from the time-lagged interactions of UQ and DQ. This leads to a smooth transition between the bandlike (UQ,DQ) distribution in marginally critical conditions (Figure 7, panel (g)) and the more constrained overcritical distribution (Figure 7, panel (d)).

So far, only correlation as a measure of linear dependency was considered. Figure 8 shows the joint distribution of LI, DQ, and LO for different arrival profiles and at particularly interesting points in time (shortly after the jump changes in the arrival profile). Only results for $\ell = 10$ are shown; the figures for $\ell = 20, 30$ do not reveal additional information. The horizontal axis represents the indices of the different

Table 5 Stationary Correlations Between UQ and DQ

λ ℓ	0.1 veh/s	0.3 veh/s	0.5 veh/s
10	0.57	0.68	0.52
20	0.45	0.76	0.50
30	0.38	0.81	0.46

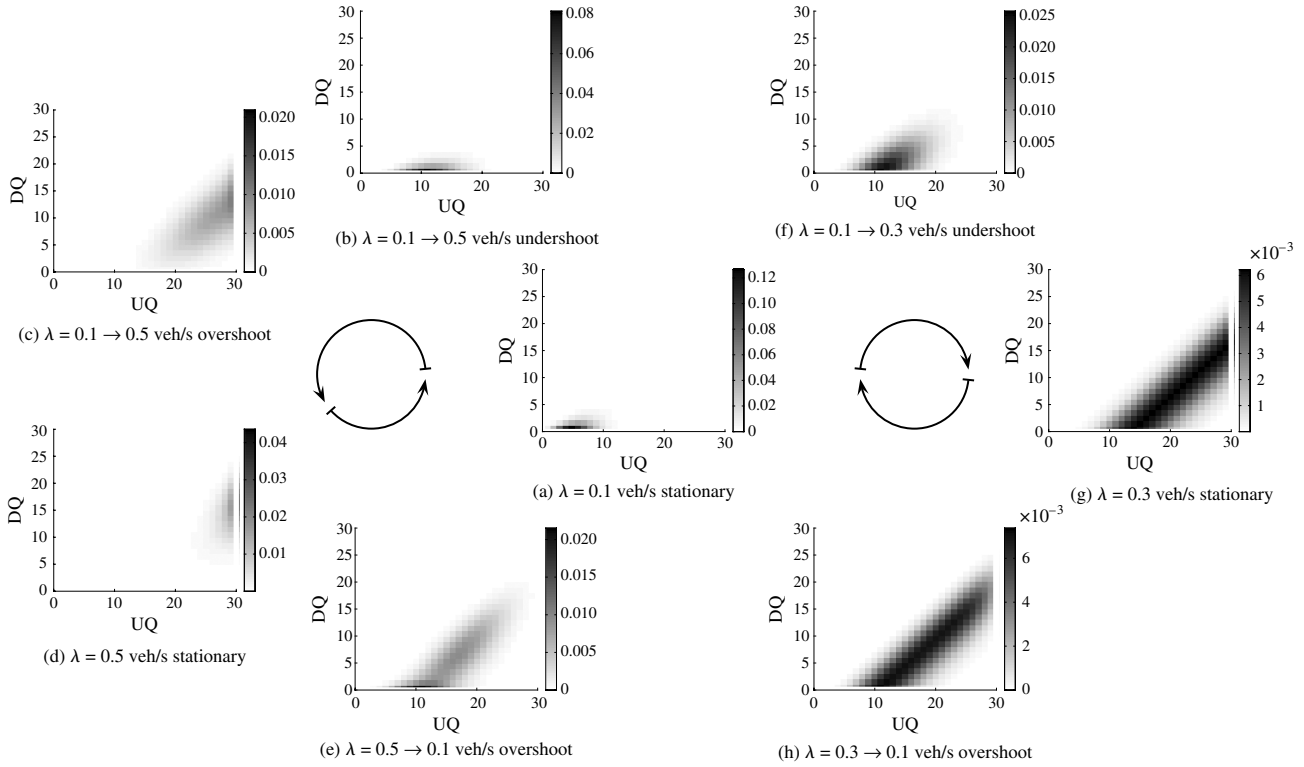


Figure 7 (UQ, DQ) Joint Distributions

Notes. Panels (a), (g), and (d) show stationary distributions for $\lambda = 0.1, 0.3,$ and 0.5 veh/s, respectively. Arranged between these panels in circles along the indicated directions are (UQ, DQ) distributions at the moments of largest under- and overshoot during the respective transients; cf. Figures 4–6. All results are obtained with the analytical model and $\ell = 30$.

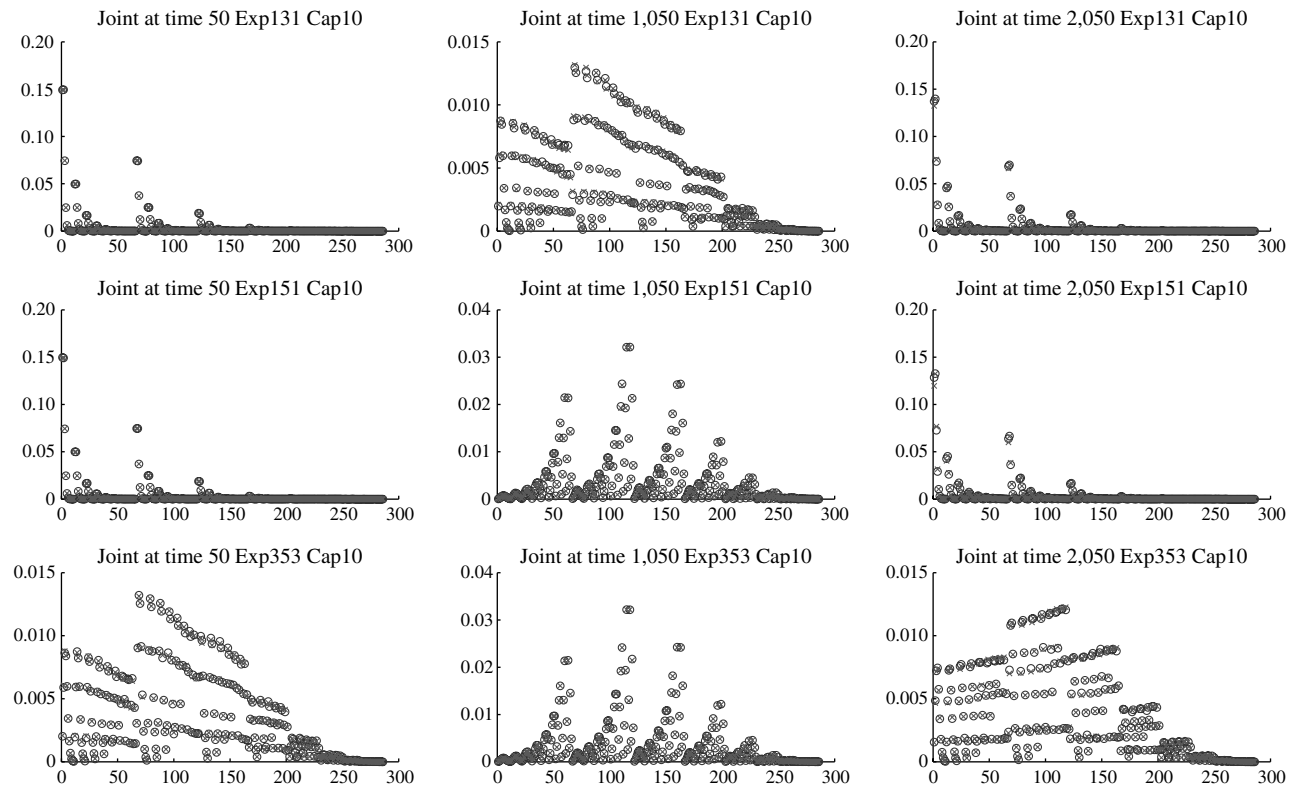


Figure 8 Joint Distribution of LI, DQ, and LO

states, and the vertical axis represents their probabilities. All feasible states of (LI, DQ, LO) are represented. One observes an almost perfect match between simulated and analytical results across all experiments.

These experiments demonstrate an extremely high precision of the analytical model when approximating an event-based microsimulation of the exact stochastic KWM model for a homogeneous link. It hence is possible to analytically capture full-link state distributions in consistency with a stochastic Newell (1993) model.

5. Summary and Outlook

This paper presents a new model for traffic flow along a linear link, which analytically captures queue length distributions. When compared with a previous approach, the new model adds a realistic dependency structure between the link's upstream and downstream boundary conditions. To maintain tractability of the new model, some simplifications are adopted, which result in a negligible loss of precision when compared with a stochastic microsimulator.

The relationship of the proposed model to the kinetic theory of traffic flow may be worth investigating further. In kinetic models, stochasticity enters at the level of individual vehicle interactions, rendering the stochastic performance of a whole link an accumulation of such interactions. The present work limits itself to (demand) stochasticity at a link's upstream end and (supply) stochasticity at its downstream end. This, in combination with the Poissonian assumption, leads to an operational but arguably simplified representation of real traffic. An effort to derive the present model from (or to link it to) kinetic theory may enable richer distributional assumptions and may also facilitate the derivation of more operational kinetic models.

Further efforts will focus on network modeling. This paper describes how dependency across a homogeneous link can be captured; previous work demonstrated how dependency across a node can be captured (Osorio, Flötteröd, and Bierlaire 2011). A logical next step is to combine these two models into an approximation of the joint queue length distributions in a complete network.

References

Ansorge R (1990) What does the entropy condition mean in traffic flow theory? *Transportation Res. Part B* 24(2):133–143.
Boel R, Mihaylova L (2006) A compositional stochastic model for real time freeway traffic simulation. *Transportation Res. Part B* 40(4):319–334.
Charypar D (2008) Efficient algorithms for the microsimulation of travel behavior in very large scenarios. Ph.D. thesis, Swiss Federal Institute of Technology Zurich, Zurich.
Corthout R, Flötteröd G, Viti F, Tampere CMJ (2012) Non-unique flows in macroscopic first-order intersection models. *Transportation Res. Part B* 46(3):343–359.

Daganzo CF (1994) The cell transmission model: A dynamic representation of highway traffic consistent with the hydrodynamic theory. *Transportation Res. Part B* 28(4):269–287.
Daganzo CF (1995) A finite difference approximation of the kinematic wave model of traffic flow. *Transportation Res. Part B* 29(4):261–276.
Daganzo CF (2005) A variational formulation of kinematic waves: Basic theory and complex boundary conditions. *Transportation Res. Part B* 39(2):187–196.
Flötteröd G, Rohde J (2011) Operational macroscopic modeling of complex urban intersections. *Transportation Res. Part B* 45(6):903–922.
Flötteröd G, Bierlaire M, Nagel K (2011) Bayesian demand calibration for dynamic traffic simulations. *Transportation Sci.* 45(4):541–561.
Helbing D (2001) Traffic and related self-driven many-particle systems. *Rev. Modern Physics* 73:1067–1141.
Jabari SE, Liu HX (2012) A stochastic model of traffic flow: Theoretical foundations. *Transportation Res. Part B* 46(1):156–174.
Larson RC, Odoni AR (1981) *Urban Operations Research* (Prentice-Hall, Englewood Cliffs, NJ).
Lebacque JP (1996) The Godunov scheme and what it means for first order traffic flow models. Lesort J-B, ed. *Proc. 13th Internat. Sympos. Transportation Traffic Theory* (Pergamon, Lyon, France), 647–667.
Lebacque JP, Khoshyaran MM (2005) First-order macroscopic traffic flow models: Intersection modeling, network modeling. Mahmassani HS, ed. *Proc. 16th Internat. Sympos. Transportation Traffic Theory* (Emerald Group Publishing, Bingley, UK), 365–386.
Lighthill MJ, Witham JB (1955) On kinematic waves II. A theory of traffic flow on long crowded roads. *Proc. Roy. Soc. A* 229(1178):317–345.
Nagel K, Nelson P (2005) A critical comparison of the kinematic-wave model with observational data. Mahmassani HS, ed. *Proc. 16th Internat. Sympos. Transportation Traffic Theory* (Emerald Group Publishing, Bingley, UK), 145–163.
Nelson P, Kumar N (2006) Point constriction, interface, and boundary conditions for kinematic-wave model. *Transportation Res. Record* 1965:60–69.
Newell GF (1993) A simplified theory of kinematic waves in highway traffic, part I: General theory. *Transportation Res. Part B* 27(4):281–287.
Osorio C, Bierlaire M (2013) A simulation-based optimization framework for urban transportation problems. *Oper. Res.* 61(6):1333–1345.
Osorio C, Flötteröd G, Bierlaire M (2011) Dynamic network loading: A stochastic differentiable model that derives link state distributions. *Transportation Res. Part B* 45(9):1410–1423.
Reibman A (1991) A splitting technique for Markov chain transient solution. Stewart WJ, ed. *Numerical Solution of Markov Chains* (Marcel Dekker, Inc., New York), 373–400.
Richards PI (1956) Shock waves on the highway. *Oper. Res.* 4(1):42–51.
Sumalee A, Zhong RX, Pan TL, Szeto WY (2011) Stochastic cell transmission model (SCTM): A stochastic dynamic traffic model for traffic state surveillance and assignment. *Transportation Res. Part B* 45(3):507–533.
Tampere CMJ, van Arem B, Hoogendoorn SP (2003) Gas-kinetic flow modeling including continuous driver behavior models. *Transportation Res. Record* 1852:231–238.
Tampere CMJ, Corthout R, Cattrysse D, Immers LH (2011) A generic class of first order node models for dynamic macroscopic simulations of traffic flows. *Transportation Res. Part B* 45(1):289–309.
Yperman I (2007) The link transmission model for dynamic network loading. Ph.D. thesis, Katolieke Universiteit Leuven, Leuven, Belgium.
Yperman I, Tampere C, Immers B (2007) A kinematic wave dynamic network loading model including intersection delays. *Proc. 86 Annual Meeting Transportation Res. Board, Washington, DC.*